MASS AND RAPIDITY DISTRIBUTIONS OF DIFFRACTIVELY AND MULTIPERIPHERALLY PRODUCED CLUSTERS

By W. Sowa

Sektion Physik, Karl-Marx-Universität, Leipzig*

(Received August 25, 1975)

The mass and rapidity distributions are derived for clusters produced according to a diffractive and a multi-Regge mechanism. The careful treatment of the kinematics is essential. The results are compared with empirical functions. Some constraints on the production mechanisms, which follow from this comparison, are investigated.

1. Introduction

Assuming that in a collision of two hadrons clusters or fireballs are produced which decay in stable hadrons, Hagedorn and Ranft [1] have described single particle spectra using the Thermodynamic Model. In this model the cluster distribution after the collision was described by means of two empirical functions. An investigation of particle correlations allows one to deduce information on the cluster production mechanism [2].

The experimental results of multiplicity distributions and correlations can be explained, if the existence of a diffractive and a non-diffractive component is supposed [3, 2]. At present two mechanisms are proposed for the cluster production within the non-diffractive component; namely the independent emission of clusters and the multiperipheral production of clusters [4–10]. Non-diffractive clusters are usually assumed to decay isotropically, while diffractive clusters decay, perhaps, anisotropically [11]. By these assumptions inclusive distributions [1, 6], inclusive [2, 5, 6, 9, 12] and semi-inclusive [7, 12] rapidity correlations, azimuthal angle correlations [9, 10] and multiplicity distributions [13] are well described. In these calculations the mass and rapidity distributions of clusters are input functions.

The aim of the present paper is to calculate the exclusive mass and rapidity distributions of diffractively and non-diffractively produced clusters in two and three body final states (clusters or stable particles). By comparing these distributions with empirical functions used in models which describe the data, we want to determine constraints on the cluster production mechanism. The first step towards this aim was the calculation by Ranft and Ranft [4] of the velocity weight function $F(\lambda)$ of the Thermodynamic Model within

* Address: Sektion Physik, Karl-Marx-Universität, Linnestrasse 5, 701 Leipzig, DDR.

the multi-Regge model. The present paper is an extension of this work. Other calculations of $F(\lambda)$ were made by Cerulus [14] using an optical model and by Celeghini and Lusanna [14] using an hydrodynamical model in which the velocity distribution is computed for the hadronic matter after the collision. A calculation using the Veneziano model was performed by Demtschenko and Kuchtin [15], who obtained a Feynman-x distribution for the missing mass similar to Ref. [4].

Further investigations of cluster production in the multi-Regge model were made by Hamer [16] and Basetto, Ranft and Ranft [17]. Matsuda, Sasaki and Uematsu [18] have calculated inclusive cluster mass and rapidity distributions using a multiperipheral model. The strong ordering limit for clusters used in this work is very useful for analytical calculations, it is, however, unrealistic, as it corresponds to a nonoverlapping of the decay products of the clusters. A multiperipheral approach to the cluster production using the Bethe–Salpeter equation was adapted by Akimov, Chernavskii, Dremin and Royzen [19].

In Section 2 a short description of the amplitude is given. The general formulae are derived in Section 3. In Section 4 the numerical results are presented. A critical discussion follows in Section 5.

2. *The amplitude*

The following amplitude is used to describe a final state with k clusters and $(n-k)$ directly produced particles (i.e. not via cluster decay; see Fig. 1)

$$|A_n(m_1^2, \ldots, m_n^2, s_1, \ldots, s_{n-1}, t_1, \ldots, t_{n-1})|^2 \sim \prod_{i=1}^{n-1} e^{a_i t_i} \left(\frac{s_i s_0}{m_i^2 m_{i+1}^2}\right)^{2\alpha_i(t_i)} \prod_{i=1}^{n} \left(\frac{m_i^2}{s_0}\right)^{\tilde{\alpha}_i(0)} . \tag{2.1}$$

The mass scale is fixed with $s_0 = 1\ \mathrm{GeV}^2$.

The third factor represents the mass dependence of the coupling functions. We consider a cluster i as the sum of all possible states with the mass m_i. Then we use the optical theorem

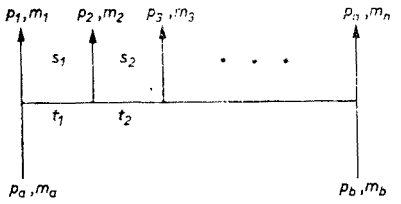

Fig. 1. The multiperipheral graph (clusters and stable particles are distinguished only by variable or fixed mass)

and write the squared coupling function as the absorptive part of the foreward scattering amplitude of the Reggeons $\alpha_{i-1}(t_{i-1})$ and $\alpha_i(t_i)$ or of one incoming particle and a Reggeon. This absorptive part for high masses has the form used in Eq. (2.1), where the t-dependence of the two triple-Regge couplings is included in the residue factor $\exp(a_i t_i)$. Assuming

duality we can use this ansatz also for low cluster masses. At limited momentum transfers t_i and high s_i and m_i^2, the propagator in Eq. (2.1) is also obtained from the Bali–Chew–Pignotti form of the Regge-propagator [20]. The expression for the propagator and the mass dependence of the vertex function can also be derived, if a summation over a multi--Regge chain is performed. This has been done by Caneschi and Pignotti [21] and by Silverman and Tan with the Chew–Goldberger–Low integral equation [22].

3. The kinematics

3.1. The mass distributions of clusters

In the following only pp-collisions are considered. If in a n-body final state k masses are variable (clusters) we obtain the following mass distribution for all clusters

$$\frac{d^k\sigma_n}{dm_{i_1}^2 \ldots dm_{i_k}^2} = c \int d\Phi_n |A_n(m_1^2, \ldots, m_n^2, s_1, \ldots s_{n-1}, t_1, \ldots, t_{n-1})|^2. \tag{3.1}$$

Here k ($k \leqslant n$) is the number of clusters which we assume to be produced along a multi--Regge chain, c is the flux factor and $d\Phi_n$ is the n-particle phase space. The mass distribution for the cluster l is therefore

$$\frac{d\sigma_n}{dm_l^2} = c \int \prod_{j \neq l}^{k} dm_{ij}^2 d\Phi_n |A_n|^2. \tag{3.2}$$

We wish to study in detail two- and three-body final states. Since the masses vary the kinematics has to be particularly carefully treated.

For a graph with $n = 2$ and one or two clusters in the final state the amplitude (2.1) is written in the following form:

$$|A_2(s, t, m_1^2, m_2^2)|^2 = B_2 e^{Dt}, \tag{3.3}$$

with

$$B_2(s, m_1^2, m_2^2) \sim \left(\frac{ss_0}{m_1^2 m_2^2}\right)^{2\alpha(0)} \left(\frac{m_1^2}{s_0}\right)^{\tilde{\alpha}_1(0)} \left(\frac{m_2^2}{s_0}\right)^{\tilde{\alpha}_2(0)},$$

$$D(s, m_1^2, m_2^2) = a_1 + 2\alpha' \ln\left(\frac{ss_0}{m_1^2 m_2^2}\right),$$

where the trajectory $\alpha(t) = \alpha(0) + \alpha' t$ is exchanged.

We obtain the mass distribution for a graph with one cluster

$$\frac{d\sigma_2}{dm_1^2} = \frac{B_2(s, m_1^2, m_2^2 = m_p^2)}{16\pi\lambda(s, m_a^2, m_b^2)} \int_{t_{\min}}^{t_{\max}} dt \exp\left[D(s, m_1^2, m_p^2)t\right],$$

and

$$\frac{d\sigma_2}{dm_1^2} = \frac{B_2(s, m_1^2, m_p^2)}{16\pi\lambda(s, m_a^2, m_b^2)D(s, m_1^2, m_p^2)} \left[e^{D(s,m^2{}_1,m^2{}_p)t_{\max}} - e^{D(s,m^2{}_1,m^2{}_p)t_{\min}}\right]. \tag{3.4}$$

For a graph with two clusters it is

$$\frac{d\sigma_2}{dm_1^2} = \frac{1}{16\pi\lambda(s, m_a^2, m_b^2)} \int\limits_{m^2{}_{\min}=(m_p+m_\pi)^2}^{(\sqrt{s}-m_1)^2} dm_2^2 \frac{B_2(s, m_1^2, m_2^2)}{D(s, m_1^2, m_2^2)} \times \left[e^{D(s,m^2{}_1,m^2{}_2)t_{\max}} - e^{D(s,m^2{}_1,m^2{}_2)t_{\min}}\right], \tag{3.5}$$

with

$$t_{\substack{\max\\\min}} = m_a^2 + m_1^2 - 2\frac{s+m_a^2-m_b^2}{2\sqrt{s}} \frac{s+m_1^2-m_2^2}{2\sqrt{s}} \pm 2\frac{\sqrt{\lambda(s, m_a^2, m_b^2)}}{2\sqrt{s}} \frac{\sqrt{\lambda(s, m_1^2, m_2^2)}}{2\sqrt{s}}, \tag{3.6}$$

and

$$\lambda(x, y, z) = x^2+y^2+z^2-2xy-2yz-2zx.$$

The term $-\exp(Dt_{\min})$ cannot be neglected here because of the variable masses. For $m_1+m_2 = \sqrt{s}$, it is $|p_{1\,\mathrm{cm}}| = 0$, i.e. $t_{\max} = t_{\min}$. Therefore the second term affects the cut-off of the distributions at the kinematical limit ($m_1+m_2 = \sqrt{s}$).

If we want to describe nonleading clusters, at least a three-particle final state has to be considered with a cluster emerging at the middle vertex. The three-body phase space integrals can be transformed to integrals over the invariants s_1, s_2, t_1, t_2. Then the t_1 and t_2 integrations can be performed analytically [23].

The amplitude for a three-body final state is written in the form

$$|A_3(s_1, s_2, t_1, t_2, m_1^2, m_2^2, m_3^2)|^2 = B_3 \exp(D_1t_1+D_2t_2),$$

$$B_3(s_1, s_2, m_1^2, m_2^2, m_3^2) \sim \left(\frac{s_1s_0}{m_1^2m_2^2}\right)^{2\alpha_1(0)} \left(\frac{s_2s_0}{m_2^2m_3^2}\right)^{2\alpha_2(0)} \left(\frac{m_1^2}{s_0}\right)^{\tilde{\alpha}_1(0)} \left(\frac{m_2^2}{s_0}\right)^{\tilde{\alpha}_2(0)} \left(\frac{m_3^2}{s_0}\right)^{\tilde{\alpha}_3(0)},$$

$$D_1(s_1, m_1^2, m_2^2) = a_1+2\alpha_1' \ln\left(\frac{s_1s_0}{m_1^2m_2^2}\right),$$

$$D_2(s_2, m_2^2, m_3^2) = a_2+2\alpha_2' \ln\left(\frac{s_2s_0}{m_2^2m_3^2}\right). \tag{3.7}$$

We get the mass distribution for the central cluster 2:

$$\frac{d\sigma_3}{dm_2^2} = \int \prod_{j\neq 2}^{3} dm_j^2 ds_1 ds_2 \frac{d\sigma_3}{ds_1 ds_2 \prod_k dm_k^2}, \tag{3.8}$$

where

$$\frac{d\sigma_3}{ds_1 ds_2 \prod_k dm_k^2} = \frac{B_3 J}{4\pi^3\lambda(s, m_a^2, m_b^2)},$$

with

$$J = 4\exp\left\{\frac{D_1}{2}\left[s_2 - s + m_a^2 + m_b^2 + m_1^2 - \frac{1}{s}(m_b^2 - m_a^2)(s_2 - m_1^2)\right]\right.$$

$$\left. + \frac{D_2}{2}\left[s_1 - s + m_a^2 + m_b^2 + m_3^2 - \frac{1}{s}(m_a^2 - m_b^2)(s_1 - m_3^2)\right]\right\} \frac{\sinh\sqrt{\lambda(s, m_a^2, m_b^2)C/s^2}}{\sqrt{C}} \tag{3.9}$$

and

$$C = D_1^2\lambda(s, s_2, m_1^2) + D_2^2\lambda(s, s_1, m_3^2) + 2D_1D_2[s(s - s_1 - s_2 - m_1^2 - m_3^2 + 2m_2^2)$$
$$-(s_1 - m_3^2)(s_2 - m_1^2)].$$

The remaining integrations over s_1, s_2 and m_i^2 have to be performed numerically.

3.2. The rapidity distributions of clusters

First we note the kinematical relations between the rapidity and the invariants. From Eq. (3.1) we obtain the rapidity distribution of a cluster j by integrating over the masses and inserting a δ-function

$$\frac{d\sigma_n}{d\eta_j} = c\int\prod_i dm_i^2 d\Phi_n |A_n|^2 \delta(\eta_j - \eta_j(s, s_k, t_k, m_k^2)). \tag{3.10}$$

The rapidity of cluster j is

$$\eta_j = \tanh^{-1}\left(\frac{p_{\parallel j}}{E_j}\right) = \cosh^{-1}\left(\frac{E_j}{\sqrt{p_{\perp j}^2 + m_j^2}}\right)\mathrm{sign}\,(p_{\parallel j}). \tag{3.11}$$

In the following we consider symmetrical distributions in negative and positive cms-rapidity and suppress the negative rapidities.

$|A_n|^2$ and $d\Phi_n$ do not depend explicitly on the rapidity η. With the help of the δ-function one other quantity can be eliminated from the set $\{s_i, t_i, m_i^2\}$.

$$\frac{d\sigma_n}{d\eta_j} = c\int\prod_i dm_i^2 d\Phi_n |A_n|^2 \frac{dv}{d\eta_j}\delta(v - v(\eta_j, \ldots)), \tag{3.12}$$

$$v \in (s_i, t_i, m_i^2).$$

In the following v and $dv/d\eta$ are computed. This should be done for leading and nonleading clusters separately. The rapidity of a leading cluster 1 is considered in a final state with arbitrary number of bodies. We are working in the cms.

The momentum transfer to the missing mass $\sqrt{s'}$ is

$$t_1 = t' = m_a^2 + m_1^2 - 2E_aE_1 + 2p_{a\parallel}p_{1\parallel},$$

$$(p_{a\parallel} = |\vec{p}_a|), \tag{3.13}$$

with

$$E_1 = \frac{s+m_1^2-s'}{2\sqrt{s}} \qquad s' = (p_2+\ \ldots\ +p_n)^2. \tag{3.14}$$

Substituting $p_{1\|}$ and E_1 in Eq. (3.11) it follows that

$$\eta_1 = \tanh^{-1}\left\{\frac{s\left[2t'-m_a^2-m_b^2+s-m_1^2\left(\frac{s+m_b^2-m_a^2}{s}\right)-s'\left(\frac{s+m_a^2-m_b^2}{s}\right)\right]}{(s+m_1^2-s')\sqrt{\lambda(s,m_a^2,m_b^2)}}\right\}. \tag{3.15}$$

Here we choose $v = m_1^2$ and with $K = \sqrt{\lambda(s,m_a^2,m_b^2)}\tanh\eta_1$ we have

$$m_1^2 = \frac{s\left[2t'-m_a^2-m_b^2+s-s'\left(\frac{s+m_a^2-m_b^2}{s}\right)\right]-(s-s')K}{K+s+m_b^2-m_a^2}. \tag{3.16}$$

The derivative is

$$\frac{dm_1^2}{d\eta_1} = -\left[\frac{s-s'+m_1^2}{\sqrt{\lambda(s,m_a^2,m_b^2)}\tanh\eta_1+s+m_b^2-m_a^2}\right]\frac{\lambda(s,m_a^2,m_b^2)}{\cosh^2\eta_1}. \tag{3.17}$$

The t'-dependence of m_1^2 and $dm_1^2/d\eta_1$ (implicit in $m_1^2(t'^2)$) prevents us from integrating over t' analytically. To avoid the connected numerical difficulties we neglect in m_1^2 the $p_\perp$ of the cluster.

$$\eta_1 = \cosh^{-1}\left(\frac{E_1}{m_1}\right) = \cosh^{-1}\left(\frac{s+m_1^2-s'}{2m_1\sqrt{s}}\right). \tag{3.18}$$

Thus we have

$$m_{1\pm}^2 = s(\cosh\eta_1 \pm \sqrt{\sinh^2\eta_1+s'/s})^2. \tag{3.19}$$

Since $m_1^2 < s$ only the negative sign of the square root is relevant. The Eqs (3.17) and (3.19) with m_{-1}^2 are needed in the calculation of the rapidity distribution (3.12).

To find the expression for the rapidity of an arbitrary central cluster c we use the following notations:

$$\begin{aligned} &p_1+\ \ldots\ +p_{c-1} = p_l, \quad p_l^2 = m_l^2, \quad (p_l+p_c)^2 = s_l, \\ &p_{c+1}+\ \ldots\ +p_n = p_r, \quad p_r^2 = m_r^2, \quad (p_c+p_r)^2 = s_r. \end{aligned} \tag{3.20}$$

In this way the problem is reduced to a quasi-three particle final state. It is

$$E_c = \frac{s+m_c^2-(p_l+p_r)^2}{2\sqrt{s}} = \frac{s_l+s_r-m_l^2-m_r^2}{2\sqrt{s}}, \tag{3.21}$$

and

$$p_{c\|} = -p_{r\|}-p_{l\|}. \tag{3.22}$$

In analogy to (3.16) we compute $p_{r\parallel}$ and $p_{l\parallel}$ via the momentum transfers t_r and t_l respectively. We obtain

$$\eta_c = \tanh^{-1}\left\{\frac{s\left[2t_r - 2t_l + (m_l^2 - m_r^2)\left(\frac{s+m_b^2-m_a^2}{s}\right) + (s_r - s_l)\left(\frac{s+m_a^2-m_b^2}{s}\right)\right]}{\sqrt{\lambda(s, m_a^2, m_b^2)}\,(s_r + s_l - m_l^2 - m_r^2)}\right\}. \tag{3.23}$$

Using the variables defined in Eqs (3.20), the rapidity of a central cluster does not depend on its mass. We choose $v = s_l$

$$s_l = \frac{2s(t_r - t_l) + (m_l^2 - m_r^2)(s + m_b^2 - m_a^2) + s_r(s + m_a^2 - m_b^2) - (s_r + m_l^2 - m_r^2)K}{K + s + m_a^2 - m_b^2}. \tag{3.24}$$

The derivative is

$$\frac{ds_l}{d\eta_c} = \frac{m_l^2 + m_r^2 - s_l - s_r}{\sqrt{\lambda(s, m_a^2, m_b^2)}\tanh\eta_c + s + m_a^2 - m_b^2}\,\frac{\sqrt{\lambda(s, m_a^2, m_b^2)}}{\cosh^2\eta_c}. \tag{3.25}$$

The t_r, t_l-dependences of s_l and $ds_l/d\eta_c$ do not allow the performance of the t_r, t_l-integrations in Eq. (3.12) analytically, as was done in Eq. (3.9). Therefore we neglect the transverse momenta of the clusters again and have

$$\cosh\eta_c = \frac{E_c}{m_c} = \frac{s_l + s_r - m_l^2 - m_r^2}{2m_c\sqrt{s}} \tag{3.26}$$

and finally

$$s_l = m_l^2 + m_r^2 - s_r - 2\sqrt{s}\,m_c\cosh\eta_c. \tag{3.27}$$

In the calculation of the rapidity distribution (3.12) Eqs (3.25) and (3.27) are used. Now we are able to write down the rapidity distributions of the graphs under consideration according to Eq. (3.12):

— *the rapidity distribution of leading clusters*

— in two-particle final states

$$\frac{d\sigma_2}{d\eta_1} = \frac{d\sigma_2}{dm_1^2}\frac{dm_1^2}{d\eta_1}, \tag{3.28}$$

$$\frac{d\sigma_2}{d\eta_1} = \int dm_2^2\,\frac{d^2\sigma_2}{dm_1^2 dm_2^2}\,\frac{dm_1^2}{d\eta_1}, \tag{3.29}$$

where $dm_1^2/d\eta_1$ is given in Eq. (3.17). There it is $s' = m_2^2$.

— in three-particle final states

$$\frac{d\sigma_3}{d\eta_1} = \int\prod_{j=2}^{3} dm_j^2 ds_1 ds_2\,\frac{d\sigma_3}{ds_1 ds_2\prod_k dm_k^2}\,\frac{dm_1^2}{d\eta_1}. \tag{3.30}$$

Here we have in Eq. (3.17) $s' = s_2$.

— *the rapidity distributions of central clusters*

$$\frac{d\sigma_3}{d\eta_2} = \int \prod_j^3 dm_j^2 ds_2 \frac{d\sigma_3}{ds_1 ds_2 \prod_k dm_k^2} \frac{ds_1}{d\eta_2}, \tag{3.31}$$

where $ds_1/d\eta_2$ is given in Eq. (3.25). There it is $m_l^2 = m_1^2$, $m_r = m_3^2$ and $s_r = s_2$, $s_l = s_1$.

The remaining integrations over the s_i and m_i^2 in Eqs (3.28)–(3.31) are performed numerically.

4. The results

4.1. The mass distributions

4.1.1. The diffractive clusters

From triple-Regge fits the missing mass distribution for single diffractive cluster production in pp-collisions is obtained [24]:

$$\frac{d\sigma}{dm^2} \sim \frac{1.2}{m^3} + \frac{0.5}{m^2}. \tag{4.1}$$

The result of the numerical calculation of the single diffractive graph corresponding to Eq. (3.4) is shown in Fig. 2 with $\alpha_P(t) = 1+0.3t$ for various energies up to $\sqrt{s} = 50$ GeV. The contribution with $\tilde{\alpha}_1(0) = 1$ (Fig. 2) is consistent with a distribution $d\sigma/dm_1^2 \sim 1/m_1^2$

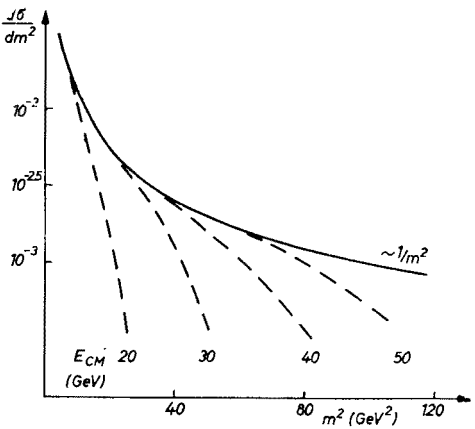

Fig. 2. The mass distribution of a single diffractive graph $\tilde{\alpha}(0) = 1.0$, $a_1 = 3$ GeV^{-2}

besides of the decrease near the kinematical limits, which we obtain due to the careful treatment of the t-integration in Eq. (3.4). The term with $\tilde{\alpha}_1(0) = 1$ corresponds to the triple-Regge-PPP-contribution in the Mueller-Regge language. The contribution with $\tilde{\alpha}_1(0) = 1/2$ (corresponding to the PPM-term) shows a decrease proportional to m^{-3}. Thus we are able to reproduce the mass distribution (4.1) with our model. Moreover,

we give an improvement to the distribution (4.1) for nonasymptotic energies because of our exact kinematics.

In calculating of the mass distribution of the cluster 1 in double diffractive events, we have taken into account four contributions:

1. $\tilde{\alpha}_1(0) = \alpha_P(0) \quad \tilde{\alpha}_2(0) = \alpha_P(0) \quad$ (PPP – PPP).
2. $\tilde{\alpha}_1(0) = \alpha_P(0) \quad \tilde{\alpha}_2(0) = \alpha_M(0) \quad$ (PPP – PPM).
3. $\tilde{\alpha}_1(0) = \alpha_M(0) \quad \tilde{\alpha}_2(0) = \alpha_P(0) \quad$ (PPM – PPP).
4. $\tilde{\alpha}_1(0) = \alpha_M(0) \quad \tilde{\alpha}_2(0) = \alpha_M(0) \quad$ (PPM – PPM).

From the first and second contribution we obtain a mass distribution proportional to m_1^{-4}, whereas the distribution according to the 3-rd and 4-th term is proportional to m_1^{-5}. Thus the mass distribution of the first cluster is not essentially affected by the vertex mass dependence of the second cluster. With this result we predict the following mass distribution for clusters produced in double diffractive events for asymptotic energies or by neglecting the exact kinematical limits for nonasymptotic energies

$$\frac{d\sigma}{dm^2} \sim \frac{C_1}{m^4} + \frac{C_2}{m^5} . \tag{4.2}$$

4.1.2. Central clusters

In the literature various cluster mass distributions are used. Pokorski and Van Hove [8] use in an independent cluster emission model the following distribution

$$\frac{d\sigma}{dm} \sim m \exp\left[- \left(\frac{m}{m_0} \right)^{\alpha} \right], \tag{4.3}$$

with $m_0 = 1$ GeV and $\alpha = 1.3$.

For a mass-rapidity distribution of central clusters in an independent cluster emission model Ranft and Ranft [7] take

$$F^{(n)}(\eta, m, s) = \frac{b^2(m-m_0) \exp\left[-b(m-m_0)\right]}{2 \ln\left(\frac{2\sqrt{s}}{nm} \right)}, \tag{4.4}$$

where n is the number of central clusters. The mass cut-off is $m_0 = 0.7$ GeV and the parameter b is 1.5 GeV^{-1}. By integration over η in the range

$$-\ln\left(\frac{2\sqrt{s}}{nm} \right) \leqslant \eta \leqslant \ln\left(\frac{2\sqrt{s}}{nm} \right)$$

it follows that the mass distribution is

$$\frac{d\sigma}{dm} \sim (m-m_0) \exp\left[-b(m-m_0)\right] \tag{4.5}$$

(see also Ref. [9]).

We have computed numerically the graph with two leading protons and one central cluster, corresponding to Eq. (3.8), where two meson-trajectories are exchanged ($\alpha_M = 0.5+t$). Of course we cannot expect a full correspondence of an exclusive distribution of one special graph with an inclusive distribution, but we should obtain an exponentially damped distribution. For a mass dependence $(m_2^2)^{\tilde{\alpha}_2(0)}$ of the central cluster vertex function an exponentially decreasing cluster mass distribution is not reached for $\tilde{\alpha}_2(0) = 1.0$ and $\tilde{\alpha}_2(0) = 0.5$ in a reasonable mass range, for residue parameters $3.0 \leqslant a \leqslant 15.0$. However, with $\tilde{\alpha}_2(0) = -1.0$ we obtain an energy independent exponentially damped distribution

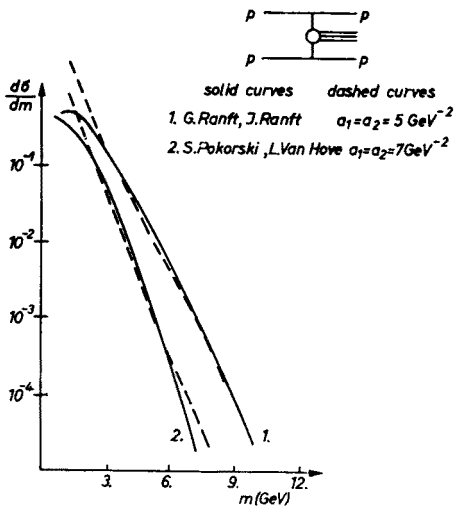

Fig. 3. The mass distribution for a central cluster for two different parameters of the residue function in comparison with the empirical functions of Pokorski and Van Hove [8] and Ranft and Ranft [7]

in the energy range $\sqrt{s} = 20...50$ GeV. With different parameters in the residue functions the tail of both distributions (4.3) and (4.5) can be represented (see Fig. 3). The somewhat arbitrary cut-off for small masses, which fixes the lowest possible cluster mass, is of course not reflected, because this graph is only the first contribution to the full multiperipheral chain.

4.2. The rapidity distributions

For central clusters Ranft and Ranft [7] (see Eq. (4.4)) and Berger [7] use a rapidity plateau with a logarithmically decreasing height in s. In the Thermodynamic Model the rapidity distributions $G(\eta, s)$ and $G_0(\eta, s)$ are used for central and leading clusters, respectively [1]. $G(\eta, s)$ has a central energy independent plateau for the energies under consideration

$$G(\eta, s) \sim \exp\left[-a \exp\left(\eta - \eta_{\max}\right)\right]\left(1 - \frac{2m_p \sinh \eta}{\sqrt{s}}\right), \tag{4.6}$$

with $a = 0.208$.

$G_0(\eta, s)$ shows an increase towards the kinematical limits. We obtain this function through transformation of the variables from function $F_0(\lambda)$, which was used earlier.

$$G_0(\eta, s) \sim \exp\left[-a_0 \frac{2m_p(\cosh\eta - 1)}{\sqrt{s} - 2m_p}\right]\left(\frac{2m_p \sinh\eta}{\sqrt{s} - 2m_p}\right), \tag{4.7}$$

with $a_0 = 4.58$.

The functions $G(\eta, s)$ and $G_0(\eta, s)$ are normalized to one cluster, so $G(\eta, s)$ is not in contradiction to a logarithmically decreasing inclusive distribution for central clusters.

4.2.1. The leading clusters

The rapidity distributions calculated from the single and the double diffractive graphs according to Eqs (3.28) and (3.29) show an exponential increase with the rapidity towards the kinematical limits for $\tilde{\alpha}(0) = \alpha_P(0)$ and $\tilde{\alpha}(0) = \alpha_M(0)$ (Fig. 4). This is in agreement with the Thermodynamic model. The curves are energy-independent or reach a limiting distribution at $\sqrt{s} \approx 50$ GeV. The parameter in the residue function has a weak influence on the slope of the distribution in the range $2.5\ \text{GeV}^{-2} \leqslant a \leqslant 7.5\ \text{GeV}^{-2}$.

For the nondiffractive component, meson-exchange is considered with $\alpha_M(t) = 0.5 + t$.

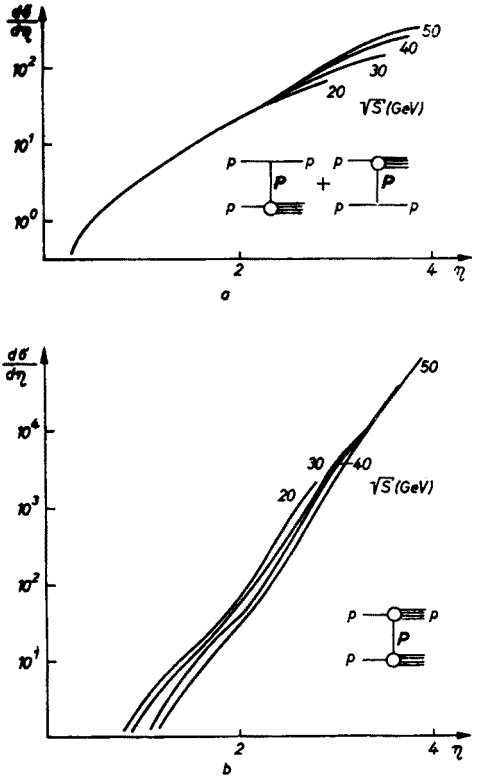

Fig. 4. The rapidity distribution for a) a single diffractively produced cluster $\tilde{\alpha}_1(0) = 1$, $a_1 = 3\ \text{GeV}^{-2}$, b) a double diffractively produced cluster $\tilde{\alpha}_1(0) = \tilde{\alpha}_2(0) = 1.0$, $a_1 = 3\ \text{GeV}^{-2}$

The rapidity distribution obtained from Eqs (3.28)–(3.30) with $\tilde{\alpha}(0) = \alpha_P(0)$ and $\tilde{\alpha}(0) = \alpha_M(0)$ shows an energy-independent plateau at the kinematical limits. Two examples are shown in Fig. 5. Because of kinematical constraints, the plateau in Fig. 5a is broader than in Fig. 5b, where an additional central pion is produced. In this case we do not obtain

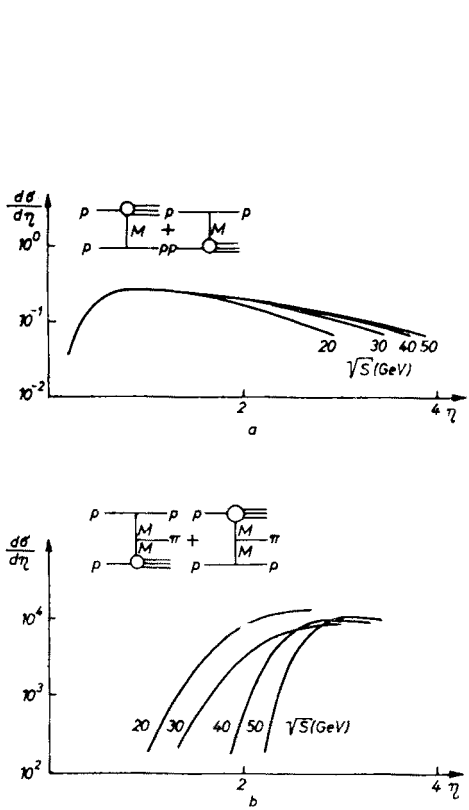

Fig. 5

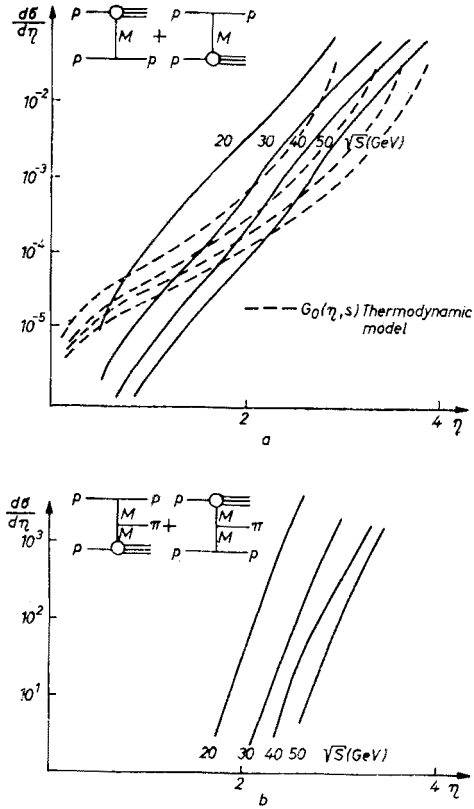

Fig. 6

Fig. 5. The rapidity distribution for a leading non-diffractive cluster with a) $\tilde{\alpha}(0) = 1.0$, $a_1 = 3.0\ \mathrm{GeV}^{-2}$, b) $\tilde{\alpha}(0) = 0.5$, $a_1 = a_2 = 5.0\ \mathrm{GeV}^{-2}$

Fig. 6. The distributions of leading clusters with $\tilde{\alpha}(0) = -1$, a) $a_1 = 3.0\ \mathrm{GeV}^{-2}$, b) $a_1 = a_2 = 5.0\ \mathrm{GeV}^{-2}$

a leading particle effect. If we choose $\tilde{\alpha}(0) = -1$ we obtain towards the kinematical limits an exponentially increasing rapidity distribution (Fig. 6). These distributions are preferred in comparison with the Thermodynamic Model.

4.2.2. The central clusters

Here also the graph with two leading protons and one central cluster is considered (Eq. (3.31)). For $\tilde{\alpha}_2(0) = 1.0$ or $\tilde{\alpha}_2(0) = 0.5$ the rapidity distribution has no plateau. The results are shown for $\tilde{\alpha}_2(0) = -1.0$ (Fig. 7). In this case we obtain a plateau in the rapidity with a somewhat stronger than logarithmically decreasing height with growing

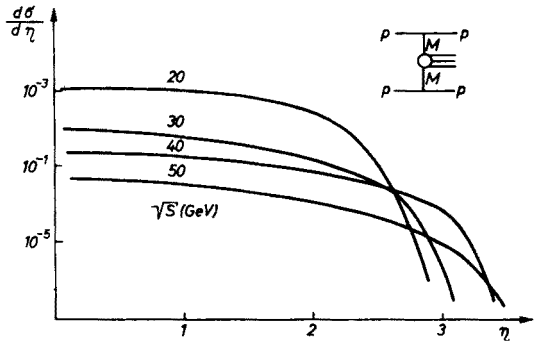

Fig. 7. The rapidity distribution for a central cluster with $\tilde{\alpha}_2(0) = -1$, ($a_1 = a_2 = 1.0\ \mathrm{GeV}^{-2}$)

energy. This may be an indication, that the contribution of this graph to the full multiperipheral chain decreases with increasing energy and graphs with more than one central cluster become more important.

5. *Discussion*

We have computed mass and rapidity distributions of clusters for various graphs. We have tried to put some constraints on the multiperipheral production mechanism of these clusters, which follow from comparison with some empirical functions.

The diffractive component is obtained in accordance with expected curves or triple-Regge fits [24], but with a careful kinematic treatment we are able to give the relevant mass range for diffractively produced clusters. For double diffractive events we predict a mass distribution (Eq. (3.5)) as well as a mass distribution for asymptotic energies (Eq. (4.2)). The diffractive component is determined by P-exchange and a vertex function, which increases as a power of the cluster mass.

The non-diffractive component is dominated by meson exchange and a vertex function, which decreases as a power of the cluster mass. This result is in agreement with the results of Hamer [16] and of Basetto, Ranft and Ranft [17], who use different arguments, such as Froissart-limit and Feynman-scaling. Since we have related the squared of the vertex function to the foreward scattering of two Reggeons, it should be equal to the product of two triple-Regge couplings $G_{\alpha_M \alpha_M \tilde{\alpha}(0)}$.

According to triple-Regge investigations for these couplings the MMP-term gives the main contribution to the non-diffractive events [25] (but only for a single leading cluster and $x \lesssim 1$). The conclusion would be $\tilde{\alpha}(0) = 1$ in contradiction to our and the above mentioned results. With a negative $\tilde{\alpha}(0)$ we are able to reproduce the empirical mass and rapidity distributions used in some models. It should be stressed, however, that we have calculated only some exclusive graphs. In particular we only have treated the first approximation to central cluster production. Our results and their comparison with the expected features give us some confidence that the treatment of the full multiperipheral chain for cluster production will not alter these features considerably.

I would like to thank Prof. G. Ranft for her suggestion to this work, for continuous comments, helpful discussions, and a critical reading of the manuscript. Furthermore, I thank Prof. J. Ranft for reading the manuscript and Dr. R. Blutner for some discussions.

REFERENCES

[1] R. Hagedorn, *Nuovo Cimento Suppl.* **3**, 147 (1965); R. Hagedorn, J. Ranft, *Nuovo Cimento Suppl.* **6**, 169 (1968); R. Hagedorn, J. Ranft, *Nucl. Phys.* **B48**, 157 (1972); J. Ranft, *Phys. Lett.* **41B**, 613 (1972).

[2] G. Ranft, J. Ranft, *Nucl. Phys.* **B53**, 217 (1973); *Phys. Lett.* **45B**, 43 (1973).

[3] A. Białas, K. Fiałkowski, K. Zalewski, *Nucl. Phys.* **B48**, 237 (1972); K. Fiałkowski, *Phys. Lett.* **41B**, 379 (1972); H. Harari, E. Rabinovici, *Phys. Lett.* **43B**, 49 (1973); K. Fiałkowski, H. I. Miettinen, *Phys. Lett.* **43B**, 61 (1973); L. Van Hove, *Phys. Lett.* **43B**, 65 (1973).

[4] G. Ranft, J. Ranft, *Phys. Lett.* **32B**, 207 (1970).

[5] P. Pirilä, S. Pokorski, *Phys. Lett.* **43B**, 502 (1973); W. Schmidt-Parzefall, *Phys. Lett.* **46B**, 399 (1973).

[6] E. L. Berger, G. C. Fox, *Phys. Lett.* **47B**, 162 (1973).

[7] G. Ranft, J. Ranft, *Phys. Lett.* **49B**, 286 (1974); *Nucl. Phys.* **B83**, 285 (1974); E. L. Berger, *Phys. Lett.* **49B**, 369 (1974); *Nucl. Phys.* **B85**, 61 (1975); A. Morel, G. Plaut, *Nucl. Phys.* **B78**, 541 (1974).

[8] S. Pokorski, L. Van Hove, *Acta Phys. Pol.* **B5**, 229 (1974).

[9] R. Blutner et al., *Nucl. Phys.* **B78**, 333 (1974).

[10] G. Ranft, J. Ranft, *Lett. Nuovo Cimento* **10**, 485 (1974); G. Ranft, J. Ranft, M. Sabau, K. G. Fadeev, A. N. Solomin, *Nucl. Phys.* **B86**, 63 (1975); G. Ranft, J. Ranft, *Nucl. Phys.* (in print).

[11] G. Ranft, J. Ranft, *Nucl. Phys.* **B69**, 285 (1974).

[12] For a review of correlations in cluster models see J. Ranft, Proc. 5th Int. Symp. on manyparticle hadrodynamics, June 1974, Leipzig—Eisenach, DDR, p. 210.

[13] J. Kripfganz, G. Ranft, J. Ranft, *Nucl. Phys.* **B56**, 205 (1973).

[14] F. Cerulus, Proc. 1 Conf. on many-particle production, Paris. E. Celeghini, L. Lusanna, Preprint: Florence, Oct. 1973.

[15] G. P. Demtschenko, W. W. Kuchtin, Preprint: IFF-73-16R.

[16] C. J. Hamer, *Phys. Rev.* **D7**, 2723 (1973).

[17] A. Basetto, G. Ranft, J. Ranft, KMU-HEP-7309.

[18] S. Matsuda, K. Sasaki, T. Uematsu, Kyoto preprints: KUNS-288; KUNS-294.

[19] V. N. Akimov, D. S. Chernavski, I. M. Dremin, I. I. Royzen, *Nucl. Phys.* **B14**, 285 (1969).

[20] N. F. Bali, G. F. Chew, A. Pignotti, *Phys. Rev.* **163**, 1572 (1967).

[21] L. Caneschi, A. Pignotti, *Phys. Rev. Lett.* **22**, 1213 (1969).

[22] D. Silverman, C.-I. Tan, *Nuovo Cimento* **2A**, 489 (1971); *Phys. Rev.* **D2**, 233 (1970).

[23] Chan Hong-Mo, K. Kajantie, G. Ranft, *Nuovo Cimento* **49**, 157 (1967).

[24] A. Capella, M. S. Chen, M. Kugler, R. D. Peccei, *Phys. Rev. Lett.* **31**, 497 (1973); A. B. Kaidalov, V. A. Khoze, Yu. F. Pirogov, N. L. Ter-Isaakyan, *Phys. Lett.* **45B**, 493 (1973); K. Abe et al., *Phys. Rev. Lett.* **31**, 1530 (1973).

[25] D. P. Roy, R. G. Roberts, RL-74-T79.